

# Glycosaminoglycanomics of Cultured Cells Using a Rapid and Sensitive LC-MS/MS Approach

Guoyun Li,<sup>†,‡,○</sup> Lingyun Li,<sup>§,‡,○</sup> Fang Tian,<sup>||</sup> Linxia Zhang,<sup>⊥</sup> Changhu Xue,<sup>†</sup> and Robert J. Linhardt<sup>\*,⊥,#,▽</sup>

<sup>†</sup>College of Food Science and Technology, Ocean University of China, Qingdao, Shandong 266003, China

<sup>‡</sup>Department of Chemistry and Chemical Biology, Center for Biotechnology and Interdisciplinary Studies, Rensselaer Polytechnic Institute, Troy, New York 12180, United States

<sup>§</sup>Wadsworth Center, New York State, Department of Health, Albany, New York 12201, United States

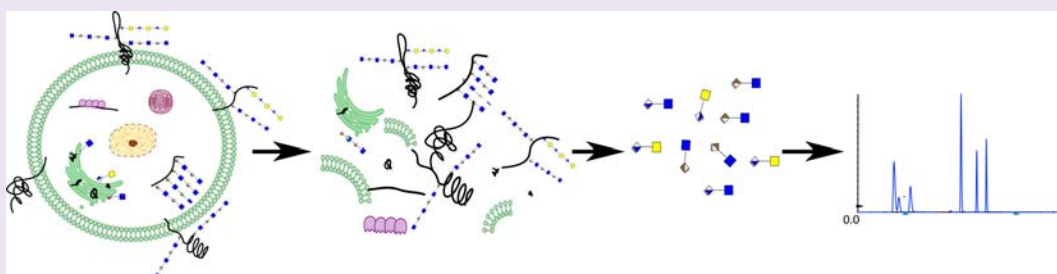
<sup>||</sup>American Type Culture Collection, Manassas, Virginia 20110, United States

<sup>⊥</sup>Biomedical Engineering, Center for Biotechnology and Interdisciplinary Studies, Rensselaer Polytechnic Institute, Troy, New York 12180, United States

<sup>#</sup>Chemical and Biological Engineering, Center for Biotechnology and Interdisciplinary Studies, Rensselaer Polytechnic Institute, Troy, New York 12180, United States

<sup>▽</sup>Biology, Center for Biotechnology and Interdisciplinary Studies, Rensselaer Polytechnic Institute, Troy, New York 12180, United States

## **S** Supporting Information



**ABSTRACT:** Glycosaminoglycans (GAGs), a family of polysaccharides widely distributed in eukaryotic cells, are responsible for a wide array of biological functions. Quantitative disaccharide compositional analysis is one of the primary ways to characterize the GAG structure. This structural analysis is typically time-consuming (1–2 weeks) and labor intensive, requiring GAG recovery and multistep purification, prior to the enzymatic/chemical digestion of GAGs, and finally their analysis. Moreover,  $10^5$ – $10^7$  cells are usually required for compositional analysis. We report a sensitive, rapid, and quantitative analysis of GAGs present in a small number of cells. Commonly studied cell lines were selected based on phenotypic properties related to the biological functions of GAGs. These cells were lysed using a commercial surfactant reagent, sonicated, and digested with polysaccharide lyases. The resulting disaccharides were recovered by centrifugal filtration, labeled with 2-aminoacridone, and analyzed by liquid chromatography (LC)-mass spectrometry (MS). Using a highly sensitive MS method, multiple reaction monitoring (MRM), the limit of detection for each disaccharide was reduced to 0.5–1.0 pg, as compared with 1.0–5.0 ng obtained using standard LC-MS analysis. Sample preparation time was reduced to 1–2 days, and the cell number required was reduced to 5000 cells for complete GAG characterization to as few as 500 cells for the characterization of the major GAG disaccharide components. Our survey of the glycosaminoglycanomes of the 20 selected cell lines reveals major differences in their GAG amounts and compositions. Structure–function relationships are explored using these data, suggesting the utility of this method in cellular glycobiology.

Glycosaminoglycans (GAGs) are a family of polysaccharides distributed in all animal cells, in organisms ranging from *C. elegans* to humans.<sup>1</sup> These GAGs are commonly found attached to core proteins, in the form of glycoconjugates called proteoglycans (PGs).<sup>2</sup> PGs, containing one or multiple GAG chains, are biosynthesized in the endoplasmic reticulum and the Golgi<sup>3</sup> and transported to the cell membrane and extracellular matrix where they perform numerous biological functions.<sup>4–6</sup> The most prominent of these functions, involving cell signaling, takes place through the interaction of

a GAG chain with protein growth factors and growth factor receptors.<sup>7–9</sup> Other critical roles of GAGs involve the binding of chemokines in chemotaxis<sup>10–12</sup> and in cellular adhesion.<sup>13,15</sup> Dysregulation of GAG biosynthesis, catabolism, and distribution can result in severe pathology and even cell and organism death.<sup>3,15</sup>

**Received:** January 7, 2015

**Accepted:** February 13, 2015

**Published:** February 13, 2015

The analysis of glycans, particularly GAGs, has trailed far behind the analysis of other biopolymers including nucleic acids and proteins. This results from the additional structural complexity of these glycans and their highly polar nature making their rapid and sensitive analysis particularly challenging. Today, even the compositional analysis of the GAG component of a cell line can require  $10^5$ – $10^7$  cells and take 1–2 weeks.<sup>16,17</sup> More sophisticated analyses, such as oligosaccharide mapping and sequencing, are only just beginning to be attempted.<sup>17–19</sup> Thus, cellular glycomics is many decades behind genomics and proteomics.

GAGs are comprised of prominent groupings, hyaluronan (HA) and heparan sulfate (HS) and the chondroitin sulfates (CSs). HA, the simplest GAG, is biosynthesized at the cell membrane and is not attached to a core protein. It has a uniform repeating disaccharide structure of  $\rightarrow 3$ -GlcNAc (1  $\rightarrow$  4) GlcA (1  $\rightarrow$  , where GlcNAc is *N*-acetyl- $\beta$ -D-glucosamine and GlcA is  $\beta$ -D-glucuronic acid. The HA GAG is a high molecular weight (>100 kDa) polydisperse polysaccharide that gives rise to a single type of unsaturated ( $\Delta$ UA) disaccharide,  $\Delta$ UA(1  $\rightarrow$  3)GlcNAc, when treated with either hyaluronan lyase or chondroitin lyase.<sup>20</sup> HS is an intermediate molecular weight (10–25 kDa) polydisperse polysaccharide found as a glycoconjugate, covalently *O*-linked to serine residues of multiple core proteins, and is the most complex GAG with a repeating disaccharide structure of  $\rightarrow 4$  GlcNAc or GlcNS or GlcN (1  $\rightarrow$  4) GlcA or IdoA (1  $\rightarrow$  , where GlcN is  $\alpha$ -D-glucosamine and GlcNS is *N*-sulfo- $\alpha$ -D-glucosamine and IdoA is  $\alpha$ -L-iduronic acid. The GlcNAc and GlcNS residues can also be modified with *O*-sulfo groups (S) substituted on their 3- and 6-hydroxyls and the IdoA and GlcA with 2-*O*-sulfo groups.<sup>21</sup> On treatment with heparin lyases, HS gives rise to eight major and several minor unsaturated disaccharides.<sup>20,22</sup> Chondroitin sulfates are comprised of repeating disaccharide units of  $\rightarrow 3$  GalNAc (1  $\rightarrow$  4) GlcA or IdoA (1  $\rightarrow$  , with *N*-acetyl- $\beta$ -D-galactosamine. This family of GAGs also contains *O*-sulfo group substitution at various positions that are designated as CS-A, CS-B, CS-C, CS-D, and CS-E.<sup>23</sup> These CS GAGs are intermediate molecular weight (~25 kDa) polydisperse polysaccharides that are *O*-linked to the serine residues of various core proteins and give rise to eight different disaccharide products when treated with chondroitin lyases.<sup>23</sup> Because of the structural similarity of disaccharide products afforded through enzymatic treatment, it is very

challenging to simultaneously identify and quantify these disaccharides from a complex biological sample matrix with a high level of both specificity and sensitivity. Liquid chromatography (LC)-tandem mass spectrometry (MS/MS) using multiple reaction monitoring (MRM) detection has been proven to be one of the most sensitive and specific methods for complex biological sample analysis.<sup>24–28</sup> LC-MS/MS using MRM detection of HS disaccharides first described by Imanari and co-workers and by Leary and Saad<sup>26,27</sup> has also been applied to patient sera and urine to study mucopolysaccharidosis.<sup>29</sup> Unfortunately, the Hypercarb column used in the LC portion of this method does not exhibit sufficient resolution to separate all of the disaccharides generated from HS and CS.

The current study describes a rapid and sensitive method for the GAG compositional analysis of cultured cells. In the current method, cells are disrupted with sonication in the presence of a surfactant and digested with polysaccharide lyases, and the resulting disaccharide products are recovered by centrifugal filtration, labeled by reductive amination and analyzed by LC-MS/MS using MRM. Once the complete recovery of cellular GAGs and their sensitive analysis by this method had been established using Chinese hamster ovary (CHO) cells, a survey of 20 commonly used human cell lines was undertaken. The glycosaminoglycanome (GAG-ome) of these cells showed remarkable differences suggesting a rich biology associated with the functional glycomics of these cell lines.

## RESULTS AND DISCUSSION

**Method Development.** Method development took place using CHO cells grown in suspension culture as previously described.<sup>30</sup> These cells were harvested and washed with phosphate buffered saline at RT. The cell pellet was collected by centrifugation, and the pellets were stored frozen prior to analysis. The optimized workflow for disaccharide analysis is presented in Figure 1. Briefly, CHO cells were suspended in a disruption reagent in a sonic bath for 10 min and incubated with a cocktail of GAG lyases for 5 h, and the disaccharides were recovered using a spin column and reductively aminated with AMAC. AMAC labeling offers several advantages including enhanced analytical selectivity for reducing sugars, improved chromatographic properties allowing optimal interaction and resolution of AMAC-labeled disaccharides on a reversed phase column without added ion-pairing reagents, and increased

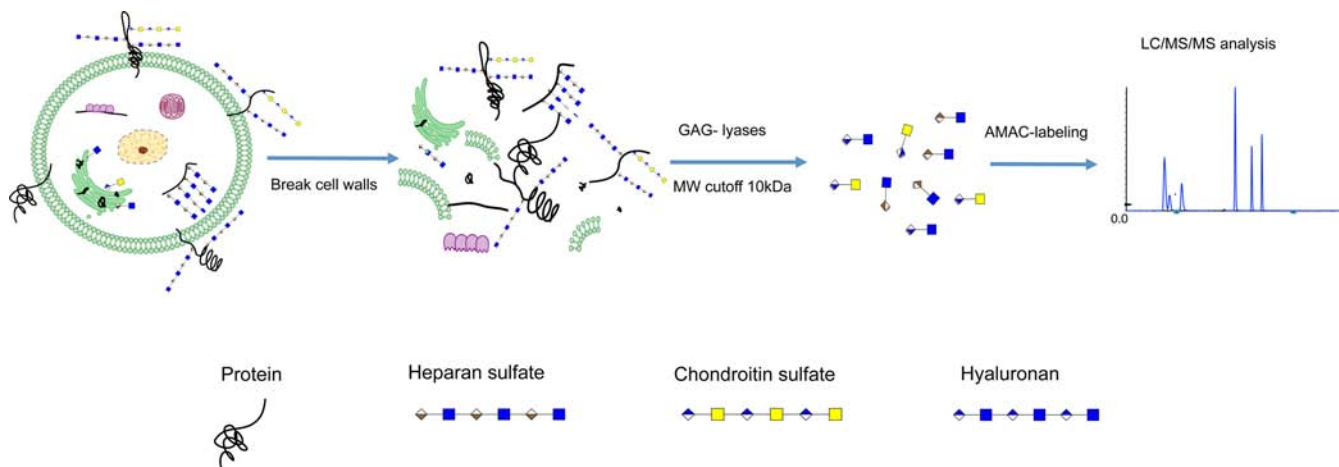


**Figure 1.** Workflow for sample preparation of AMAC-labeled GAGs-derived disaccharides from the cell samples.

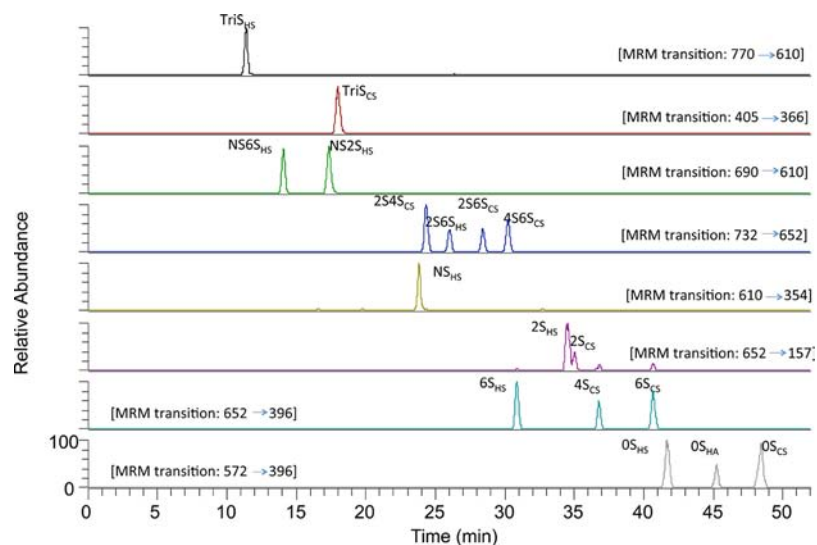


**Figure 2.** MRM ion chromatograms of 17 HS/CS/HA disaccharide standards ( $100 \text{ pg } \mu\text{L}^{-1}$  standards and  $4.0 \text{ } \mu\text{L}$  sample injected on the C18 reverse-phase column).

hydrophobicity of AMAC-labeled disaccharides improving ionization efficiency and increasing detection sensitivity. The AMAC-labeled disaccharides (Supporting Information Figures 1–13) were analyzed by LC-MS/MS using MRM.

MS/MS analysis (Supporting Information Figures 1–13) demonstrated that some isobaric AMAC-labeled disaccharides showed unique fragments while others did not, requiring their LC separation before MRM analysis to achieve the high sensitivity and specificity in the analysis of complex biological samples. MRM could be used effectively for the analysis of a mixture of 17 AMAC-labeled disaccharide standards ( $4 \text{ } \mu\text{L}$  of  $100 \text{ pg } \mu\text{L}^{-1}$  each; Figure 2). Optimized instrument conditions and MRM transitions used in these analyses are provided in Supporting Information Table 1. The calculated LOD was from  $0.5 \text{ pg}$  to  $1.0 \text{ pg}$ , much less than the LOD ( $1.0$  to  $5.0 \text{ ng}$ ) obtained using standard LC-MS analysis.<sup>31</sup> The CHO cell GAG composition has been intensively studied, particularly by our laboratory, and CHO cells contain  $\sim 10$ -fold more CS than HS, making it challenging to obtain an HS disaccharide composition with less than  $10^7$  cells.<sup>30,31</sup> Therefore, to test the recovery in our new MRM method, we undertook the analysis of CHO cell HS. The MRM disaccharide analysis of the HS GAGs from the CHO cell sample shows that seven of the eight HS disaccharides were present (Supporting Information Figure 14) and provided analysis comparable with those obtained using a standard LC-MS method that required  $10^7$  CHO cells (Supporting Information Table 2). Moreover, a linearity study of the MRM method demonstrated that it could be used to obtain identical HS disaccharide compositional analysis for samples containing cell numbers ranging between 500 and 100 000 CHO cells (Supporting Information Figure 15). A low signal-to-noise afforded high quality MRM data even using 500 CHO cells (Supporting Information Figure 14).

**GAG Differences of 20 Cell Lines Studied.** We initially surveyed structural data across the entire sample set of 20 cell lines (Table 1 and Supporting Information Table 3) without considering the biological influence or phenotypic impact for the observed structural differences. The differences considered included GAG type and amount (Figure 3), sulfation level, and disaccharide composition (Figure 4A–C and Supporting Information Table 4).

**Table 1. Human Cell Lines Analyzed by LC-MS/MS**

cell line	ATCC #	tissue source	physiology	cell growth properties
HL-60	CCL-240	blood and lymph	leukemia	suspension
Raji	CCL-86	blood and lymph	Burkitt's lymphoma	suspension
KG-1	CCL-246	blood and lymph	acute myelogenous leukemia	suspension
U-2 OS	HTB-96	bone	osteosarcoma	adhesion
MG-63	CRL-1427	bone	osteosarcoma	adhesion
HS-5	CRL-11882	bone marrow/stroma	normal, nontumor	adhesion
T-47D	HTB-133	breast	carcinoma	adhesion
MDA-MB-231	HTB-26	breast	adenocarcinoma	adhesion
MDA-MB-134-VI	HTB-23	breast	ductal carcinoma	adhesion
MCF 10A	CRL-10317	breast	normal, nontumor	adhesion
WiDr	CCL-218	colon	adenocarcinoma	adhesion
COLO 320DM	CCL-220	colon	adenocarcinoma	adhesion
BEAS-2B	CRL-9609	lung	normal, nontumor	adhesion
NCI-H1417	CRL-5869	lung	small cell carcinoma	suspension
HCN-2	CRL-10742	neuron, cortical	normal, nontumor	adhesion
Hs746T	HTB-135	stomach	carcinoma	adhesion
KATO III	HTB-103	stomach	adenocarcinoma	adhesion
SNU-5	CRL-5973	stomach	undifferentiated adenocarcinoma	suspension
SNU-16	CRL-5974	stomach	undifferentiated adenocarcinoma	suspension
HUV-EC-C	CRL-1730	vein, umbilical cord	normal, nontumor	adhesion

Initial profiling examined cell lines that contained the maximum and minimum amounts of hyaluronan (HA), chondroitin sulfate (CS), and heparan sulfate (HS). The HA, CS, and HS contents of the 20 cell lines averaged and ranged from 155 (avg)  $0.1$ – $1936 \text{ ng}/10^6$  cells, 86 (avg)  $2.3$ – $879 \text{ ng}/10^6$  cells, and 93 (avg)  $0.4$ – $536 \text{ ng}/10^6$  cells, respectively (Figure 3). The stromal cells and a stomach carcinoma cell line (HS-5 and Hs746T) contained very high levels of HA (12- and 5-fold above

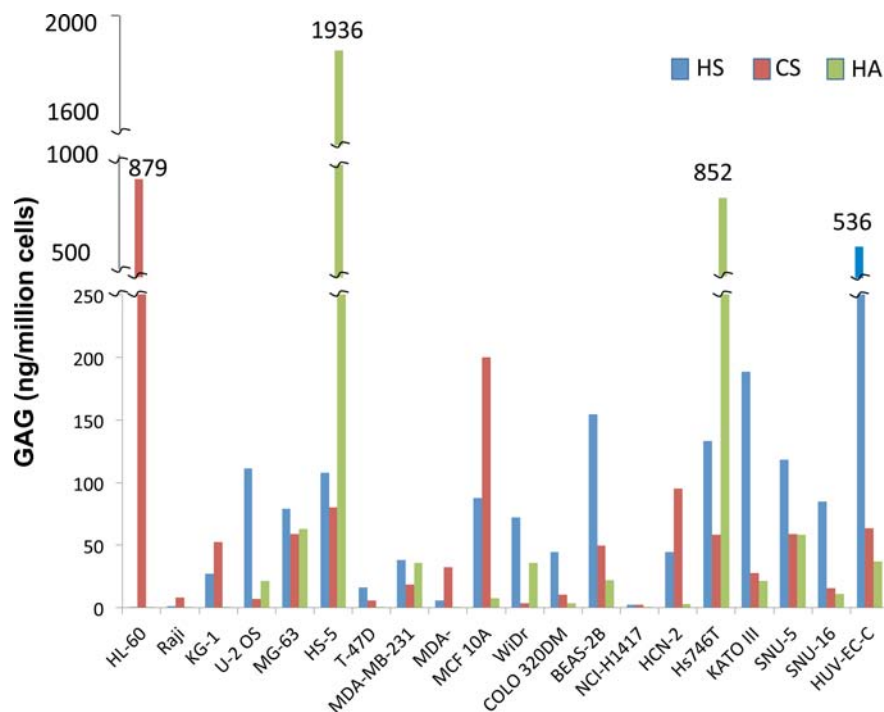


**Figure 3.** Amounts of GAGs produced by 20 human cell lines. The analytical error for each GAG is <5%.

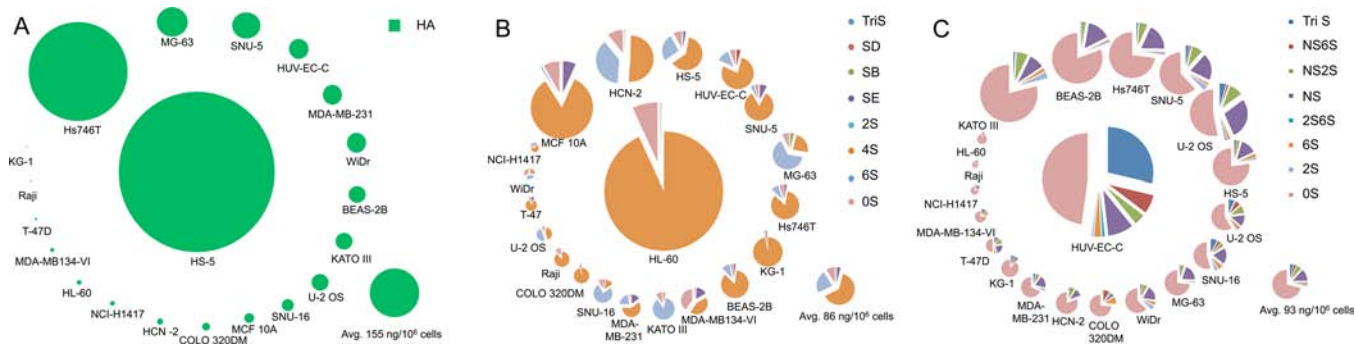


**Figure 4.** Disaccharide composition of GAGs produced by 20 human cell lines. (A) Amount of HA. (B) Amount and disaccharide composition of CS. (C) Amount and disaccharide composition of HS. The size of the pie charts represents the total amount of the GAG in the specific type of the cells. The analytical error for each disaccharide is <5%.

the average value) with nine cell lines (MCF 10A, T-47D, COLO 320DM, NCI-H1417, HL-60, Raji, MDA-MB-134-VI, HCN-2, and KG-1) showing either little or no HA. The leukemia cell line (HL-60) contained high levels of CS (10-fold above the average value) with the small cell lung carcinoma and colon adenocarcinoma lines (NCI-H1417 and WiDr) showing the lowest amount of CS (37- and 26-fold below the average value). The vascular endothelial cell line (HUV-EC-C) contained high levels of HS (6-fold above the average value) with leukemia, lymphoma, and small lung carcinoma lines (HL-60, Raji, NCI-H1417) showing the lowest amount of HS (233- to 44-fold below the average value).

The compositional analysis of CS and HS GAGs can offer some additional insight into the GAG-omes of the different cell lines (Figure 4b and c). The cell lines having the highest and lowest sulfation levels in CS are small cell lung carcinoma (NCI-H1417) and breast ductal carcinoma (MDA-MB-134-VI), respectively, and the cell lines having the highest and the lowest sulfation levels in HS are the vascular endothelial (HUV-EC-C) and the leukemia line (HL-60), respectively. The most complex

CS structure was found in the breast ductal carcinoma cell line (MDA-MB-134-VI), with the least complex CS structures in the macrophage cell line (KG-1). Chondroitin sulfates are commonly classified as types A and B (4S), C (6S), and E (4S6S), and those cell lines containing the most of each of these three types are colon adenocarcinoma (COLO 320DM), stomach adenocarcinoma (KATO-III), and breast ductal carcinoma (MDA-MB-134-VI), respectively, and the least of each type are stomach adenocarcinoma (KATO-III), leukemia (HL-60), and vascular endothelial cell line (HUV-EC-C), respectively. The most complex HS structure was found in the vascular endothelial cell line (HUV-EC-C) with the least complex HS structures in the leukemia cells (HL-60). As expected, the HS present in the 20 cell lines studied was more structurally diverse than was the CS. Only two cell lines had easily measurable quantities of only four HS disaccharides with eight of the cell lines having all eight HS disaccharides. In contrast, seven cell lines had easily measurable quantities of only four CS disaccharides with five cell lines having six of the eight CS disaccharides, and one CS disaccharide, 2S, was absent from all 20 cell lines.

**Differences of Cell Lines and Their GAG-omes.** Next, we examined biological properties across the entire sample set including developmental origin and phenotype in an effort to correlate these biological properties to GAG structural differences. Cell lines were selected to test GAG-relevant cell growth properties and GAG-relevant signaling pathways and to examine other relevant cell types (Supporting Information Table 3). Of the 20 cell lines studied, six were normal (Table 1) and 14 cancerous (Table 1).

From the standpoint of development, eight cell lines are of endoderm origin, seven cell lines are of mesoderm origin, and five cell lines are of ectoderm origin (Supporting Information Table 3). The cell lines of ectoderm origin were the most similar to one another with low levels of HA, all with the dominant form of CS being CS-A, and all with average or slightly below average levels of HS. This similarity is not surprising since four of the five lines of ectoderm origin are derived from breast tissue. The cell lines from mesoderm origin and from endoderm origin were both highly variable in GAG content and composition. Interestingly, the mesoderm lines showed both the highest and lowest HA contents. One line of endoderm origin, small cell lung cancer line (NCI-H1417), had among the lowest levels of all of the GAGs. This line's HS had an above average content of NS and OS and a below average amount of the other six HS disaccharides. The CS in this line showed above average SD, SE, and 4S with all the other CS disaccharides observed in below average amounts with OS at the lowest level observed in all 20 cell lines.

The one endothelial cell line (HUV-EC-C) had an endothelial morphology, with mesodermal and lateral visceral origin, and displayed the highest level of HS of all 20 lines examined, with below average levels of CS and HA. The HS in this line was very atypical, showing the highest content of TriS and 2S6S, and the CS in this line showed the highest content of SD. HUV-EC-C cells are the classic endothelial cell line used for *in vitro* testing. They are a good measure of systemic (e.g., nonpulmonary) endothelial cells. Since HUV-EC-C cells are not a transformed cell line, they have greater relevance to human endothelial cells. The one lymphocyte cell line (Raji) of lymphatic system origin had one of the lowest amounts of HS and HA. The HS in this line had one of the highest contents of OS, heparosan. The macrophage cell line (KG-1) of myeloblastic morphology and of lymphatic system origin had one of the lowest levels of HA, the simplest CS structure consisting primarily of 4S and an HS with a high content of OS (heparosan). The one leukemia cell line (HL-60) of lymphocyte cell type and blood origin contained the highest level of CS, a simple structure of primarily 4S, and among the lowest levels of HA. This line had a very small amount of HS that consisted primarily of OS (heparosan). The one stromal cell line (HS-5) of fibroblast morphology and of mesodermal and intermedial mesonephorous origin was the richest of all 20 cell lines in HA. But had CS and HS in very average amounts and of typical contents. The neuron cell line (HCN-2) of neuronal morphology and ectodermal/neural tube origin had a low HA content with average levels of HS and CS of typical composition.

GAG chains are known to play important roles in cellular adhesion.<sup>2,5,6</sup> There were 14 adherent cell lines (Table 1) and six suspension cell lines (Table 1). All of the suspension cell lines had below average levels of HA (Figure 4a) with all, except SNU-5, being among the lowest levels measured in the 20 cell lines. Two of the adherent cell lines showed extremely high levels of HA (Hs746T and HS-5) with the remaining showing lower levels of HA with T-47D and MDA-MB-134-VI showing

among the lowest HA levels measured in the 20 cell lines. Less of a pattern was observed in CS content (Figure 4b), and the suspension cell lines contained both lines having the highest and lowest CS contents. The CS disaccharide composition of the suspension cell lines had below average levels of all observed disaccharides except for the 4S disaccharide. The HS levels (Figure 4c) of the suspension lines were generally below average and contained the three cell lines having the lowest levels of HS (NCI-H1417, HL-60, and Raji). The HS disaccharide composition of the suspension cell lines was slightly lower in sulfated disaccharides and slightly enriched in OS (heparosan).<sup>7–10</sup>

GAG chains play important roles in growth factor signaling,<sup>7–10</sup> and their composition changes in cancer.<sup>32–38</sup> A comparison of the normal and cancer cell lines (Table 1) showed the normal cell lines with similar and relatively high levels of CS, compared to lower levels of CS observed in nearly all the cancer cell lines. No remarkable differences in HA and HS content were observed between the normal and cancer cell lines.

The one ductal carcinoma cell line (MDA-MB-134-VI) of epithelial morphology and of ectodermal/epidermis origin showed low levels of all of the GAGs (Figures 3 and 4). The CS from this cell line was very atypical. It was the only CS containing TriS and showed the highest level of SE and the highest level of OS and one of the lowest levels of 6S. This line's HS had a below average content of OS and NS (the lowest observed in an HS from any of the 20 cell lines) and slightly above average amounts of the other six HS disaccharides. Disaccharides with 6-*O*-sulfo groups were present in the ductal carcinoma cell line at twice the level found in the average of the 20 lines studied. Previous *in vitro* studies on breast ductal carcinoma cell lines showed that sulfation levels in HS decreased cell migration<sup>32</sup> and inhibited fibroblast growth factor (FGF)-2 interactions,<sup>33</sup> which inhibited growth. However, in studying the FGF-2/HS-proteoglycan interactions, Delehedde and co-workers also found that decreasing the HS sulfation was not exclusively inhibitory and was, in fact, a growth promoter, within certain limitations, for one of the two breast cancer cell lines studied.<sup>33</sup> Changing HS sulfation patterns have also been linked to changing inhibition of heparanase, an enzyme that is a potent metastatic agent. Evaluation of normal and tumor biopsy samples from breast cancer patients showed that HS from tumors in lethal cancers contained twice the level of 6-*O*-sulfo disaccharides.<sup>34</sup> The *SULF-1* gene encodes for sulfatase-1, which cleaves 6-*O*-sulfo groups from HS, and this loss of 6-*O*-sulfo groups inhibits cancer growth.<sup>35–37</sup> Down-regulation of *SULF-1* in breast cancer cells results in increased autocrine activation of the EGFR–ERK pathway.<sup>38</sup>

The one colorectal adenocarcinoma cell line (COLO 320DM) with round and refractile morphology had low levels of all GAGs. It had an HS with the highest content of NS6S and 6S and a CS with the highest amount of 4S and one of the lowest amounts of 6S content. The two osteosarcoma cell lines (U-2 OS and MG-63), one of epithelial and one of fibroblast morphologies with the origin of bone, have slightly low HA, and the line of epithelial cell morphology (U-2 OS) has a low amount of CS.

The four gastric cell cancer lines contained three with epithelial (Hs746T, SNU-5, and SNU-16) and one with spherical morphology (KATO III) and were all of endodermal and digestive tube origin. Two were undifferentiated adenocarcinomas that grew in suspension (SNU-5 and SNU-16). While the two undifferentiated adenocarcinomas (SNU-5 and SNU-16) showed reduced amounts of HA, the stomach carcinoma (Hs746T), which grew as an adherent line, showed elevated levels of HA. All the

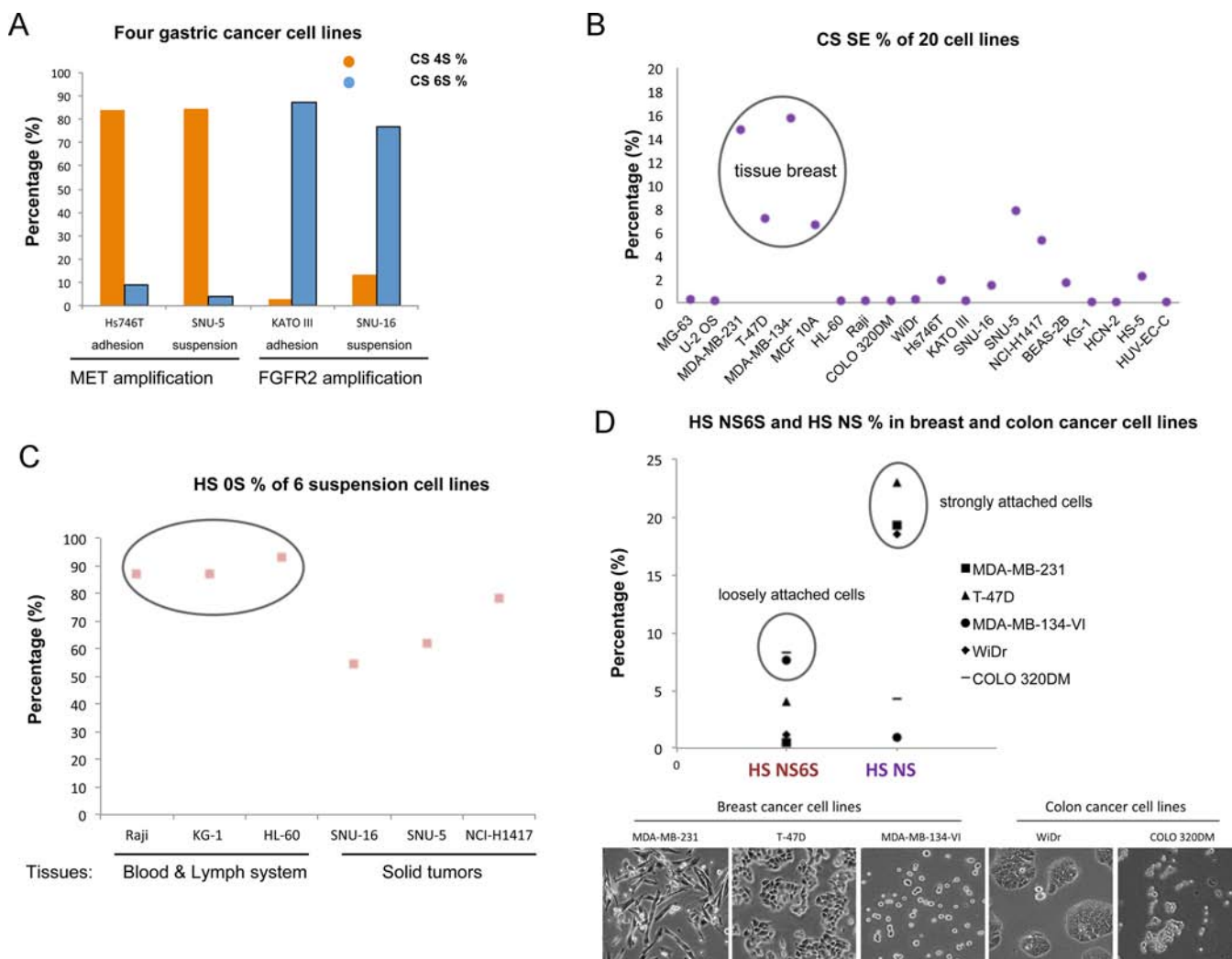


**Figure 5.** Functional glycosaminoglycanomics of human cell lines. (A) Comparison of chondroitin 4- and 6-sulfates in four gastric cancer cell lines. (B) Elevation of chondroitin sulfate E in breast tissues. (C) Elevated levels of unsulfated heparan sulfate in six suspension cell lines. (D) Differences in the percentages of heparan sulfate NS6S and NS sequences in loosely and strongly adherent cells.

gastric cell cancer lines showed average amounts of HS and below average amounts of CS. The CS disaccharide composition of the four gastric cancer cell lines, two showing adhesion (Hs746T and KATO III) and two suspension lines (SNU-5 and SNU-16), were next analyzed (Figure 5a). Interestingly, the content percentages of 4S and 6S within the total CS content were not related with the cell growth properties. Instead, the 4S and 6S compositions correlated with growth factor receptor expression (Supporting Information Table 3). The hepatocyte growth factor receptor (MET) and fibroblast growth factor receptor-2 (FGFR2) are both receptor tyrosine kinases that transduce signals from the extracellular matrix into the cytoplasm by binding to related growth factors.<sup>39,40</sup> These regulate many physiological processes including proliferation, differentiation, scattering, morphogenesis, and survival. The two cell lines with MET gene amplification showed over 80% of 4S CS composition and a low percentage of 6S (Figure 5a). In contrast, the two cell lines with FGFR-2 expression showed a low percentage of 4S CS and a high percentage of 6S. Chondroitin sulfate has recently been shown to support signaling through the MET pathway<sup>41</sup> as well as signaling through FGFR.<sup>42</sup>

Breast tissue derived cell lines, which include three cancer cell lines (T-47D, MDA-MB-231, and MDA-MB-134-VI) and

a normal cell line (MCF 10A), show elevated percentages of SE CS compared to the remaining 16 cell lines (Figure 5b). This suggests a tissue specific composition feature in CS unique to breast tissue derived cells, since the 20 cell lines included in this study many represent different cell adhesion properties, disease types, and cell morphology.

Six suspension cell lines (NCI-H1417, HL-60, Raji, SNU-5, SNU-16, and KG-1) were examined in this study (Figure 5c). Three of these were isolated from leukemia and lymphoma (HL-60, Raji and KG-1), and the other three lines were from solid tumors. It is interesting that the three cell lines from the blood and lymph system had the highest compositions of HS OS among the tested 20 cell lines, and they were higher than that of the other suspension cell lines developed from the solid tumors.

We also explored the impact of cell morphology and adhesion properties on the GAGs expression and composition (Figure 5d). Five cell lines from breast cancer and colon cancer corresponding to loosely and strongly attached cell lines were examined. HS levels of NS6S were highest in loosely attached cell lines (COLO 320DM and MDA-MB-134-VI). In contrast, the HS levels of NS were highest in strongly attached cells. The GAG levels of these two HS subunits clearly show a correlation with cell growth properties of these lines.

This study applies a recent innovation in MRM for the study of glycosaminoglycanomics of 20 commonly used human cell lines. The recovery, isolation, quantification, and compositional analysis of cellular GAGs were initially demonstrated on CHO cells having a well-characterized GAG-ome, established and validated using more routine analytical methods. The structural glycosaminoglycanomic analysis of the human cell lines leads to an improved understanding of glycosaminoglycan function and represents the first step in developing a structure–function relationship for this important class of biopolymers.

## METHODS

The Chinese hamster ovary (CHO, type S) cells were from Invitrogen and were prepared for analysis as previously described.<sup>30</sup> The 20 human cell lines were from ATCC (Table 1). The cell lines were received in a frozen cryopreservation medium (0.3–18 million cells mL<sup>-1</sup>). Immediately after thawing, the cells used for analysis were pelleted by centrifugation, and the cryopreservation medium was removed. The cell pellet was then rinsed twice with phosphate buffered saline (PBS) and stored frozen until analysis. Each cell type (corresponding from 10 000 to 100 000 cells) was disrupted by adding 100  $\mu$ L of BugBuster protein extraction reagent (Novagen, Inc.) and placed in a sonic bath for 10 min at RT. Following which, 400  $\mu$ L of digesting buffer (20 mM ammonium acetate, 1 mM calcium chloride, pH 7.0) was added in the tube. The cocktail of GAG-lyases (heparin lyases 1, 2, and 3, chondroitinase ABC, and ACII (40 mU/each enzyme) was added, and the mixture was incubated for 5 h at 35 °C. The resulting disaccharides were recovered by centrifugal filtration using a 10-kDa molecular weight cutoff membrane, freeze-dried, and the GAG-derived disaccharide samples together with unsaturated disaccharides standards then labeled by reductive amination with 2-aminoacridone (AMAC).<sup>17</sup> LC-MS was performed with a triple quadrupole mass spectrometer (TSQ Quantum Ultra, Thermo Inc.) running at the Multiple Reaction Monitoring (MRM) mode. The separation was carried out with an Agilent 1200 HPLC separation system on a Poroshell 120 C18 column (3.0  $\times$  150 mm, 2.7  $\mu$ m, Agilent, USA) at 45 °C. Eluent A was water/methanol (85:15) v/v, and eluent B was water/methanol (35:65) v/v. Both eluents contained 50 mM ammonium acetate with pH adjusted to 6.5 with acetic acid. Solution A was flowed (100  $\mu$ L min<sup>-1</sup>) through the column for 5 min followed by linear gradients 0–12% solution B from 5 to 10 min, and 12%–25% solution B from 10 to 35 min. The final optimized conditions and collision energies for the all of the disaccharides MRM transitions are listed in Supporting Information Table 2.

Additional experimental procedures are presented in the Supporting Information.

## ASSOCIATED CONTENT

### Supporting Information

Additional information includes additional experimental procedures, figures showing mass spectral analyses, limit of detection data, a representative sample analysis, MRM parameters, additional information on the cell lines analyzed, and tabular disaccharide compositional data of all 20 cell lines. This material is available free of charge via the Internet <http://pubs.acs.com>.

## AUTHOR INFORMATION

### Corresponding Author

\*E-mail: [linhar@rpi.edu](mailto:linhar@rpi.edu).

### Author Contributions

<sup>○</sup>Equal contributors

### Notes

The authors declare no competing financial interest.

## ACKNOWLEDGMENTS

The work was supported by grants from the National Institutes of Health in the form of grants GM38060, GM090127, HL096972, and HL10172. G.L. was supported by the China Scholarship Council and Program for Changjiang Scholars and Innovative Research Team in University (IRT1188). The authors are grateful to Professor L. Ligon for her critical reading of this paper.

## REFERENCES

- (1) DeAngelis, P. L., Liu, J., and Linhardt, R. J. (2013) Chemoenzymatic synthesis of glycosaminoglycans: re-creating, re-modeling and re-designing nature's longest or most complex carbohydrate chains. *Glycobiology* 23, 764–777.
- (2) Couchman, J. R., and Pataki, C. A. (2012) An introduction to proteoglycans and their localization. *J. Histochem. Cytochem.* 60, 885–897.
- (3) Esko, J. D., and Selleck, S. B. (2002) Order out of chaos: assembly of ligand binding sites in heparan sulfate. *Annu. Rev. Biochem.* 71, 435–471.
- (4) Gasimli, L., Linhardt, R. J., and Dordick, J. S. (2012) Proteoglycans in stem cells. *Biotechnol. Appl. Biochem.* 59, 65–76.
- (5) Nastase, M. V., Iozzo, R. V., and Schaefer, L. (2014) Key roles for the small leucine-rich proteoglycans in renal and pulmonary pathophysiology. *Biochim. Biophys. Acta* 1840, 2460–2470.
- (6) Wight, T. N., Kinsella, M. G., Evanko, S. P., Potter-Perigo, S., and Merrilees, M. J. (2014) Versican and the regulation of cell phenotype in disease. *Biochim. Biophys. Acta* 1840, 2441–2451.
- (7) Sterner, E., Masuko, S., Li, G., Li, L., Green, D. E., Otto, N. J., Xu, Y., DeAngelis, P. L., Liu, J., Dordick, J. S., and Linhardt, R. J. (2014) Fibroblast growth factor-based signaling through synthetic heparan sulfate blocks copolymers studied using high cell density three-dimensional cell printing. *J. Biol. Chem.* 289, 9754–9765.
- (8) Ibrahim, O. A., Zhang, F., Hrstka, S. C., Mohammadi, M., and Linhardt, R. J. (2004) Kinetic model for FGF, FGFR, and proteoglycan signal transduction complex assembly. *Biochemistry* 43, 4724–4730.
- (9) Schlessinger, J., Plotnikov, A. N., Ibrahim, O. A., Eliseenkova, A. V., Yeh, B. K., Yayon, A., Linhardt, R. J., and Mohammadi, M. (2000) Crystal structure of a ternary FGF-FGFR-heparin complex reveals a dual role for heparin in FGFR binding and dimerization. *Mol. Cell* 6, 743–750.
- (10) Wang, X., Sharp, J. S., Handel, T. M., and Prestegard, J. H. (2013) Chemokine oligomerization in cell signaling and migration. *Prog. Mol. Biol. Transl. Sci.* 117, 531–578.
- (11) Rot, A. (2010) Chemokine patterning by glycosaminoglycans and receptors. *Front Biosci. (Landmark Ed.)* 15, 645–660.
- (12) Linhardt, R. J., and Toida, T. (2004) Role of glycosaminoglycans in cellular communication. *Acc. Chem. Res.* 37, 431–438.
- (13) Cohen, M., Joester, D., Geiger, B., and Addadi, L. (2004) Spatial and temporal sequence of events in cell adhesion: from molecular recognition to focal adhesion assembly. *ChemBiochem.* 5, 1393–1399.
- (14) Xian, X., Gopal, S., and Couchman, J. R. (2010) Syndecans as receptors and organizers of the extracellular matrix. *Cell. Tissue Res.* 339, 31–46.
- (15) Lawrence, R., Brown, J. R., Lorey, F., Dickson, P. I., Crawford, B. E., and Esko, J. D. (2014) Glycan-based biomarkers for mucopolysaccharidoses. *Mol. Genet. Metab.* 111, 73–83.
- (16) Skidmore, M. A., Guimond, S. E., Dumax-Vorzet, A. F., Yates, E. A., and Turnbull, J. E. (2010) Disaccharide compositional analysis of heparan sulfate and heparin polysaccharides using UV or high-sensitivity fluorescence (BODIPY) detection. *Nat. Protoc.* 5, 1983–1992.
- (17) Volpi, N., Galeotti, F., Yang, B., and Linhardt, R. J. (2014) Analysis of glycosaminoglycan-derived, precolumn, 2-aminoacridone-labeled disaccharides with LC-fluorescence and LC-MS detection. *Nat. Protoc.* 9, 541–558.
- (18) Ly, M., Leach, F. E., 3rd, Laremore, T. N., Toida, T., Amster, I. J., and Linhardt, R. J. (2011) The proteoglycan bikunin has a defined sequence. *Nat. Chem. Biol.* 7, 827–833.

- (19) Ly, M., Laremore, T. N., and Linhardt, R. J. (2010) Proteoglycomics: recent progress and future challenges. *OMICS* 14, 389–399.
- (20) Linhardt, R. J. (1994) Analysis of glycosaminoglycans with polysaccharide lyases. *Current Protocols in Molecular Biology Analysis of Glycoconjugates* (Varki, A., Ed.), pp 17.13.17–17.13.32, Wiley Interscience, Boston.
- (21) Linhardt, R. J. (2003) Heparin: Structure and activity. *J. Med. Chem.* 46, 2551–2554.
- (22) Militsopoulou, M., Lamari, F. N., Hjerpe, A., and Karamanos, N. K. (2002) Determination of twelve heparin- and heparan sulfate-derived disaccharides as 2-aminoacridone derivatives by capillary zone electrophoresis using ultraviolet and laser-induced fluorescence detection. *Electrophoresis* 23, 1104–1109.
- (23) Sugahara, K., Mikami, T., Uyama, T., Mizuguchi, S., Nomura, K., and Kitagawa, H. (2003) Recent advances in the structural biology of chondroitin sulfate and dermatan sulfate. *Curr. Opin. Struct. Biol.* 13, 612–620.
- (24) Oguma, T., Toyoda, T., Toida, T., and Imanari, T. (2001) Analytical method of chondroitin/dermatan sulfates using high performance liquid chromatography/turbo ionspray ionization mass spectrometry: Application to analyses of the tumor tissue sections on glass slides. *Biomed. Chromatogr.* 15, 356–362.
- (25) Oguma, T., Toyoda, T., Toida, T., and Imanari, T. (2001) Analytical method for keratan sulfates by high-performance liquid chromatography/turbo-ionspray tandem mass spectrometry. *Anal. Biochem.* 290, 68–73.
- (26) Oguma, T., Toyoda, T., Toida, T., and Imanari, T. (2001) Analytical method of heparan sulfates using high-performance liquid chromatography turbo-ionspray ionization tandem mass spectrometry. *J. Chromatogr. B* 754, 153–159.
- (27) Saad, O. M., and Leary, J. A. (2003) Compositional analysis and quantification of heparin and heparan sulfate by electrospray ionization ion trap mass spectrometry. *Anal. Chem.* 75, 2985–2995.
- (28) Tomatsu, S., Shimada, T., Mason, R. W., Kelly, J., LaMarr, W. A., Yasuda, E., Shibata, Y., Futatsumori, H., Montañó, A. M., Yamaguchi, S., Suzuki, Y., Orii, T. (2014) Assay for glycosaminoglycans by tandem mass spectrometry and its applications. *J. Anal. Bioanal. Technol.* S2:006. doi:10.4172/2155-9872.S2-006.
- (29) Oguma, T., Tomatsu, S., Montano, A. M., and Okazaki, O. (2007) Analytical method for the determination of disaccharides derived from keratan, heparan, and dermatan sulfates in human serum and plasma by high-performance liquid chromatography/turbo ionspray ionization tandem mass spectrometry. *Anal. Biochem.* 368, 79–86.
- (30) Datta, P., Li, G., Yang, B., Zhao, X., Baik, J.-Y., Gemmill, T. R., Sharfstein, S. T., and Linhardt, R. J. (2013) Bioengineered Chinese hamster ovary cells with Golgi-targeted 3-O-sulfotransferase-1 biosynthesize heparan sulfate with an antithrombin binding site. *J. Biol. Chem.* 288, 37308–37318.
- (31) Yang, B., Weyers, A., Baik, J.-Y., Sterner, E., Sharfstein, S., Mousa, S. A., Zhang, F., Dordick, J. S., and Linhardt, R. J. (2011) Ultraperformance ion-pairing liquid chromatography with on-line electrospray ion trap mass spectrometry for heparin disaccharide analysis. *Anal. Biochem.* 415, 59–66.
- (32) Guo, C. H., Koo, C. Y., Bay, B. H., Tan, P. H., and Yip, G. W. (2007) Comparison of the effects of differentially sulphated bovine kidney- and porcine intestine-derived heparan sulphate on breast carcinoma cellular behaviour. *Int. J. Oncol.* 31, 1415–1423.
- (33) Delehedde, M., Deudon, E., Boilly, B., and Hondermarck, H. (1996) Heparan sulfate proteoglycans play a dual role in regulating fibroblast growth factor-2 mitogenic activity in human breast cancer cells. *Exp. Cell. Res.* 229, 398–406.
- (34) Weyers, A., Yang, B., Yoon, D. S., Park, J.-H., Zhang, F., Lee, K. B., and Linhardt, R. J. (2012) A structural analysis of glycosaminoglycans from lethal and non-lethal breast cancer tissues: Towards a novel class of theragnostics for personalized medicine in oncology. *Omics* 16, 79–89.
- (35) Lai, J. P., Chien, J. R., Moser, D. R., Staub, J. K., Aderca, I., Montoya, D. P., Matthews, T. A., Nagorney, D. M., Cunningham, J. M., Smith, D. I., Greene, E. L., Shridhar, V., and Roberts, L. R. (2004) hSulf1 sulfatase promotes apoptosis of hepatocellular cancer cells by decreasing heparin binding growth factor signaling. *Gastroenterology* 126, 231–248.
- (36) Abiatari, I., Kleeff, J., Li, J., Felix, K., Buchler, M. W., and Friess, H. (2006) HSulf-1 regulates growth and invasion of pancreatic cancer cells. *J. Clin. Pathol.* 59, 1052–1058.
- (37) Narita, K., Staub, J., Chien, J., Meyer, K., Bauer, M., Friedl, A., Ramakrishnan, S., and Shridhar, V. (2006) HSulf-1 Inhibits angiogenesis and tumorigenesis *in vivo*. *Cancer Res.* 66, 6025–6032.
- (38) Narita, K., Chien, J., Mullany, S. A., Staub, J., Qian, X., Lingle, W. L., and Shridhar, V. (2007) Loss of HSulf-1 expression enhances autocrine signaling mediated by amphiregulin in breast cancer. *J. Biol. Chem.* 282, 14413–14420.
- (39) Kemp, L. E., Mulloy, B., and Gherardi, E. (2006) Signalling by HGF/SF and Met: the role of heparan sulphate co-receptors. *Biochem. Soc. Trans.* 34, 414–417.
- (40) Ornitz, D. M. (2000) FGFs, heparan sulfate and FGFRs: complex interactions essential for development. *Bioessays* 22, 108–112.
- (41) Hashiguchi, T., Kobayashi, T., Fongmoon, D., Shetty, A. K., Mizumoto, S., Miyamoto, N., Nakamura, T., Yamada, S., and Sugahara, K. (2011) Demonstration of the hepatocyte growth factor signaling pathway in the *in vitro* neurogenic activity of chondroitin sulfate from ray fish cartilage. *Biochim. Biophys. Acta* 1810, 406–413.
- (42) Sterner, E., Meli, L., Kwon, S. J., Dordick, J. S., and Linhardt, R. J. (2013) FGF-FGFR signaling mediated through glycosaminoglycans in microtiter plate and cell-based microarray platforms. *Biochemistry* 52, 9009–9019.